

Performance of High-Speed 4/2 Switched Reluctance Motor

Dong-Hee Lee* and Jin-Woo Ahn[†]

Abstract – The current study presents the design and performance of a novel 4/2 switched reluctance motor (SRM) for a high-speed air blower. With a comparative study of some rotor structures for a high-speed drive, a stepper-type rotor is optimized to produce a continuous torque and a low torque ripple. Rotor pole arc is modified to have a wide continuous output torque region, and air gap is determined to develop less torque ripple. The rotor radius is determined to reduce torque ripple with a reiterative FEM analysis. The designed rotor has three regions: short uniform, long uniform, and non-uniform air-gap region. The positive torque region is wider than a conventional 4/2 SRM without any torque dead zone. A prototype is tested and the efficiency is up to 72[%] at 30,000[rpm], 600[w] output.

Keywords: High Speed, 4/2 SRM, Non-uniform air gap, Asymmetric inductance profile

1. Introduction

Switched reluctance motor (SRM) has inherent mechanical strength and simple structure. This mechanical structure is suitable for harsh environments, high temperature, and high-speed applications [1]-[4]. SRMs are also much investigated for high-speed applications [4]-[15]. The low numbers of stator and rotor pole are very effective in reducing core loss at the high-speed region. As such, most high-speed drives use a 6/2 and a 4/2 structure [6]-[10]. The 6/2 SRM is a three-phase motor with an electrical frequency thrice that of the mechanical frequency. In comparison, the 4/2 type is a two-phase motor with an electrical frequency twice that of the mechanical frequency. With regard to cost and core loss, a two-phase 4/2 type is considered for a high-speed drive in the current study.

The conventional two-phase 4/2 SRM is a very simple power circuit and has the advantage of a core loss due to the low electrical frequency at the same speed. However, the output torque of a conventional two-phase 4/2 SRM has a high torque ripple and a torque dead zone, which are drawbacks in practical applications. Some rotor structures are addressed to reduce torque ripple and torque dead zone. With regard to torque characteristics and manufacturing process, the base model of high-speed drive is selected as a stepper-type rotor.

The proposed high-speed SRM is designed for a high-speed air blower controlled by air pressure and air flow rate. The motor speed varies according to air pressure and flow rate. Moreover, the torque ripple is very important to reduce air flow pulsation in the wide speed range.

Based on the stepper-type rotor, the shape of the rotor

[†] Corresponding Author: Department of Mechatronics Engineering, Kyungshung University, Korea. (jwahn@ks.ac.kr)

* Department of Mechatronics Engineering, Kyungshung University, Korea. (leedh@ks.ac.kr)

Received: September 1, 2010; Accepted: April 18, 2011

pole is reiteratively optimized to reduce torque ripple with a continuous output torque. The output torque profile is changed according to the shape of the rotor pole. The designed motor has three air-gap regions which are dissimilar to a conventional rotor type. Furthermore, the non-uniform air-gap regions can produce a wide positive torque region and a low torque ripple.

The experimental results are compared with the analysis and simulation results.

2. Characteristics of High-Speed 4/2 SRM

2.1 Conventional 4/2 SRM

Studies are conducted on SRMs for many applications. Generally, a 6/4 and a 12/8 SRM are applied to conventional industry applications. Moreover, a 6/2 and a 4/2 are investigated for high-speed drive due to their low iron loss and simple power circuits [3]-[4]. A 6/2 type has three times the electrical frequency of the mechanical frequency whereas a 4/2 type has twice the electrical frequency. Furthermore, a 4/2 type is two-phase drive, and its power circuit is simpler than that of a three-phase 6/2 SRM. For these reasons, the prototype SRM for a high-speed air blower is selected to be the 4/2 SRM.

Torque production in SRM involves an alignment tendency of stator and rotor pole to obtain maximum flux, i.e., minimum reluctance when the stator windings are excited. Energy conversion from electrical energy to mechanical energy on the rotor shaft is explained using the electromechanical energy conversion principle. Output energy is equal to the increase of co-energy $\Delta W'(\theta, I)$, as shown in Fig. 1, because the rotor rotates from an unaligned position to an aligned position [2-4].

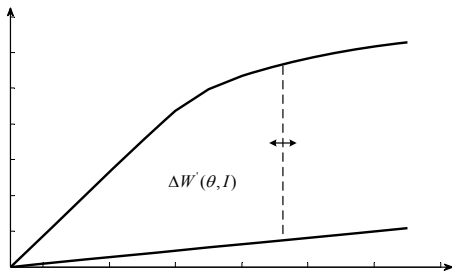


Fig. 1. Flux linkage versus mmf characteristic

Air-gap torque is calculated by (1):

$$T_e = \frac{\delta w'(\theta, i)}{\delta \theta} \quad (1)$$

Torque is also calculated by (2):

$$T_e = \frac{1}{2} i^2 \frac{dL(\theta, i)}{d\theta}, \quad (2)$$

where $L(\theta, i)$, which is the function of rotor position and current, is the inductance.

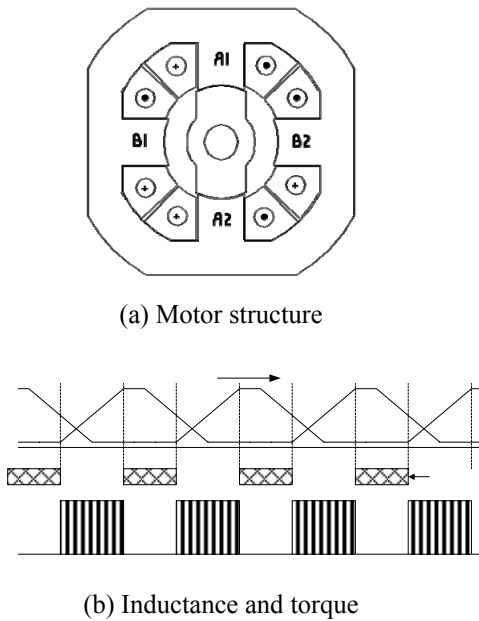


Fig. 2. Conventional 4/2 SRM

Fig. 2 shows a conventional 4/2 SRM and its torque characteristics. As shown in the figure, a conventional two-phase 4/2 SRM has symmetric inductance, and the positive torque can be produced during a positive slope of inductance. The positive slope of inductance does not overlap between two phases. As such, the output torque has a torque dead zone between two phases. In this torque dead zone, self-starting is impossible and mechanical vibration is very serious due to the high torque ripple. To reduce torque dead zone, some rotor types have been studied [4-15].

2.2 Advanced Model of High-Speed 4/2 SRM

Figs. 3, 4, and 5 show advanced models of the high-speed 4/2 SRM [5, 12, 13]. Dissimilar to a conventional 4/2 SRM, the advanced models have a wide rotor pole arc to obtain the wide positive torque region. The advanced types are designed for one-directional applications such as pump and blower. Therefore, these models have an asymmetric inductance profile which has a wide positive torque region with torque overlap between two phases and a short negative torque region. The asymmetric inductance profile is a good choice for one-directional application in a two-phase SRM.

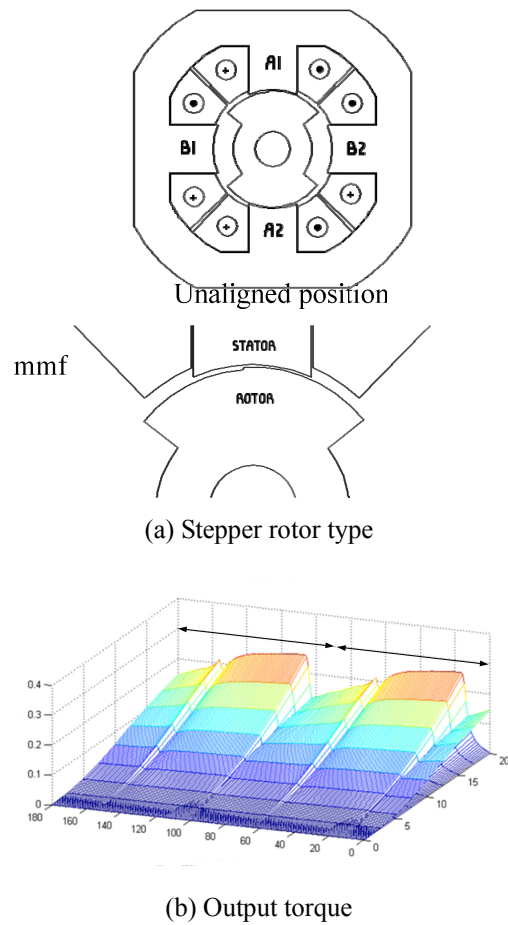
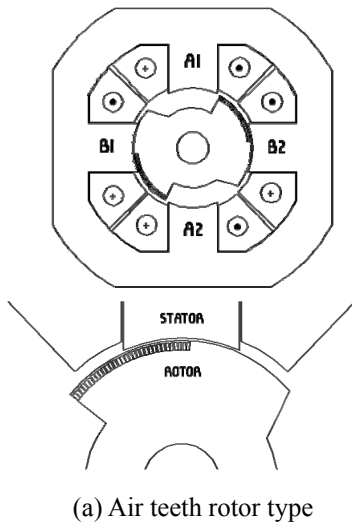


Fig. 3. Stepper rotor type 4/2 SRM

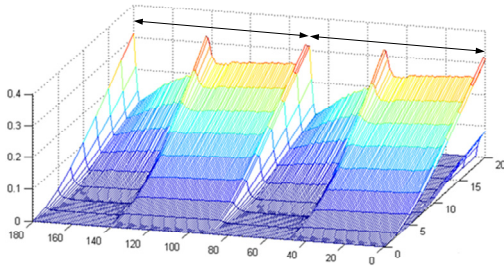
The stepper-type rotor shown in Fig. 3 has a two-level air gap [5-11]. When the rotor is the starting point of the aligned position, the motor produces low torque through the long air-gap path. When the edge of the stator pole is matched to the short air gap from the stepper point, larger flux can pass the rotor structure. This flux can produce higher torque than a short air-gap region. As shown in Fig. 3(b), the stepper model can produce a continuous torque, but it has higher torque ripple around the stepper region due to the sudden flux change.

Fig. 4 shows an air teeth rotor type and torque

characteristic [12]. The air teeth rotor type has two regions: teeth hole and conventional uniform region. In the air teeth region, the reluctance is different from the conventional region due to the air teeth. Moreover, the saturated flux in the air teeth can produce a smooth torque. Similar to the stepper rotor type, the air teeth type can produce a continuous torque, but torque ripple around the air teeth region is very high. Furthermore, the main disadvantage of the air teeth type rotor is its manufacturing difficulty. The air teeth are very small for adding a distributed flux path, and the small air teeth structure is difficult to realize in a practical system.



(a) Air teeth rotor type

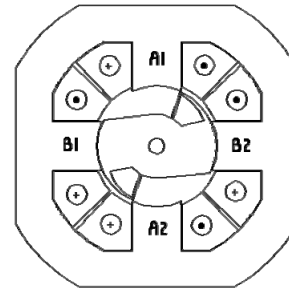


(b) Output torque

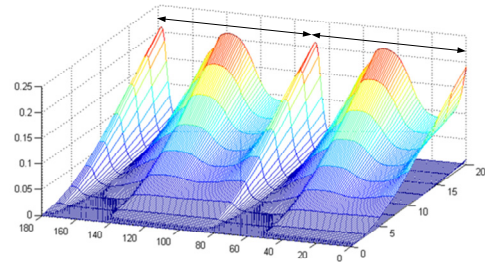
Fig. 4. Air teeth rotor type 4/2 SRM

Fig. 5 shows another rotor structure to obtain a wide torque region [13-15]. The inserted air hole can produce a saturated flux path and add additional reluctance. As shown in Fig. 5(b), the output torque is continuous but the torque ripple is much serious than those of previous models. The air hole shape should be optimized to reduce the torque ripple. However, the optimization of air hole shape is not easy with the consideration of saturation effects.

In the current study, a high-speed 4/2 SRM is designed for an air blower with 30,000[rpm] speed. With the considerations of manufacturing and optimization of torque ripple, the base model is selected as the stepper-type rotor.



(a) Air hole rotor type



(b) Output torque

Fig. 5. Air hole rotor type 4/2 SRM

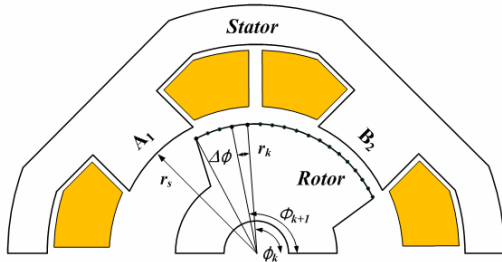
The stepper-type rotor is very simple and it can produce a wide positive torque. The torque ripple is suppressed by modifying the shape of the stepped rotor.

3. Proposed Design Process of 4/2 SRM

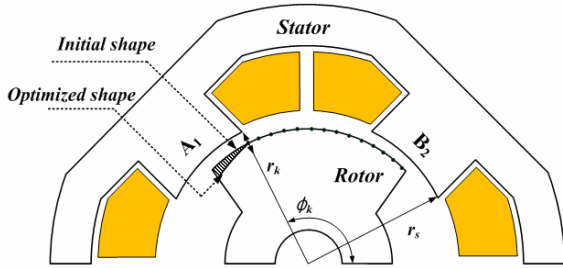
The rotor pole arc is made wider than the stator pole pitch to obtain a continuous torque with overlap region. As stated previously, the output torque is dependent on the reluctance of the magnetic circuit, which is dominantly determined by the air gap between the stator and the rotor pole. Dissimilar to the stepper rotor type, the continuous non-uniform air-gap rotor is considered to reduce torque ripple around the stepper region in the proposed 4/2 SRM. Furthermore, the continuous non-uniform air gap is optimized by FEM analysis according to the torque ripple. To optimize the air gap, the outer radius of the rotor is described by the radius and angle data in a polar coordinate (r_k, ϕ_k) is fixed to the rotor.

Fig. 6 shows the initial optimization model of the rotor shape and optimization process. As shown in Fig. 6(a), the envelope of the rotor pole is divided by n-nodes. The outer radius of the rotor is connected to each node coordinated as radius and angle. In each node, the air gap can be obtained by the inner radius of the stator pole and the outer radius on each node. At the initial condition, the output torque is calculated by FEM analysis. Torque data are then compared with the desired value and restriction condition of torque ripple. If the torque ripple is higher than the desired condition in the optimizing node, the radius of the

node is adjusted to match the condition. If the torque ripple is satisfied with the condition, the next node is optimized after the shifting angle $\Delta\phi$. The variable air gap at k -th node is determined by the $r_s - r_k$, and the k -th radius r_k is changed to reduce torque ripple in the limited band. At the k -th node, the output torque is higher than the desired one, and the radius r_k is decreased to reduce the output torque. Moreover, if the output torque is lower than the desired one, the radius r_k is increased to increase the output torque. The maximum radius is limited by the minimum air gap.



(a) Initial model for optimization



(b) Optimization process

Fig. 6. Reiterative rotor optimization process

Fig. 7 shows a flowchart for the rotor shape optimization in the proposed algorithm. In Fig. 6, the initial conditions are minimum air gap, accepted torque error $T_{err}[\%]$ according to average torque T_{avg} , node numbers, and shift step angle $\Delta\phi$. In this paper, shift step angle is 1[deg] and accepted torque error is set to 2[%]. The rated output torque is set as 0.2[Nm] for a 600[W] high-speed air blower system with a target speed of 30,000[rpm]. In general, fringing flux, when the rotor is optimized at k -th node, will vary because the $(k+1)$ -th node is being optimized. This means that optimization of the next nodes will change previous torques calculated previously. Furthermore, because air-gap flux dominates fringing fluxes, the fringing effect can be ignored, and the optimization of nodes is treated to be independent of each other.

Fig. 8 and Table 1 show the proposed rotor shape of high-speed 4/2 SRM and its specifications, respectively.

Fig. 9 shows an analyzed inductance and torque profile of the designed motor. As shown in the figure, the motor has an asymmetric inductance characteristic which can produce a wide positive and a short negative torque region.

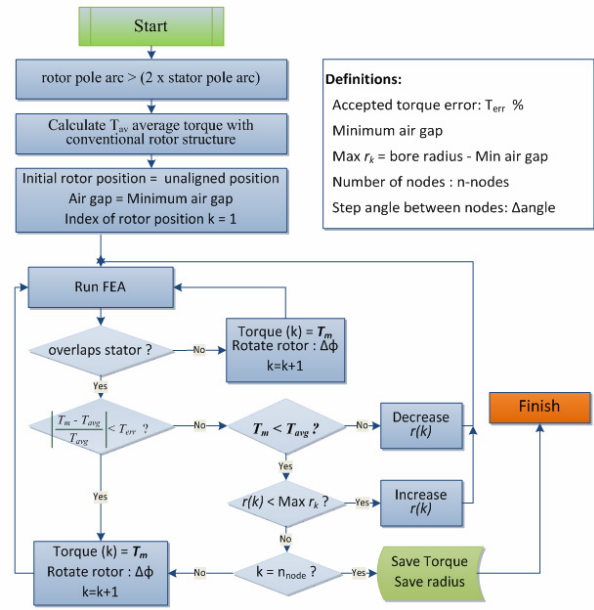
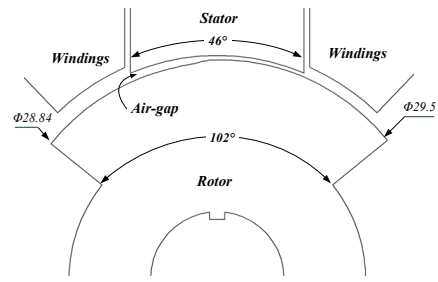


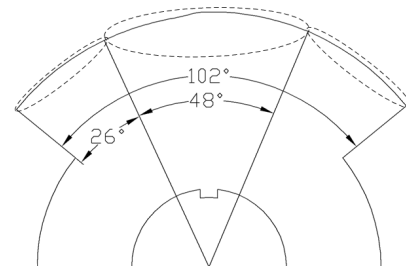
Fig. 7. Flowchart for rotor shape optimization

Table 1. Specifications of the proposed 4/2 SRM

Parameters	Value	Parameters	Value
Output power	600[W]	Average Torque	0.2[Nm]
Converter Input	220[Vac]	Stator/Rotor Poles	4 / 2
Rated speed	30,000[rpm]	Rated current	7[A]
Bore Diameter	30[mm]	Stator Outer Dia.	80[mm]
Stack Length	30[mm]	Minimum Air gap	0.25[mm]
Stator Pole Arc	46[°]	Rotor Pole Arc	102[°]
Rph	0.5[Ω]	Lmin	2[mH]



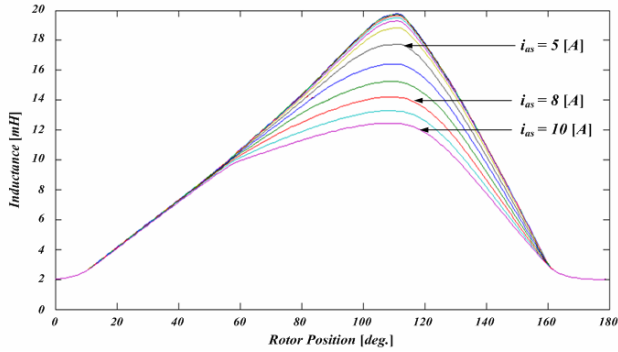
(a) Determined rotor shape



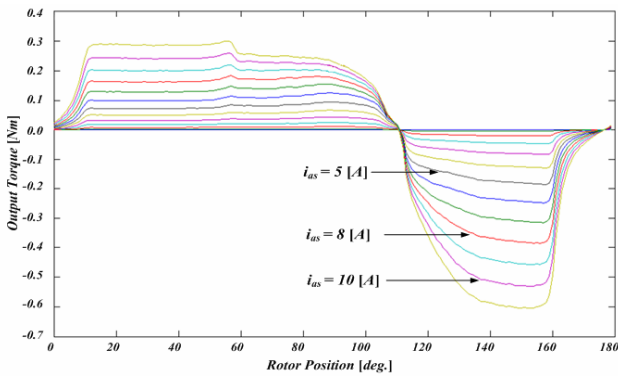
(b) Optimized rotor details

Fig. 8. Optimized rotor pole shape

With consideration of the saturation effect, the proposed motor is optimized at the 7[A] phase current, which is the rated current of the motor. The inductance profile is linear and the output torque is constant in a light load. In a heavy load, the torque ripple around the center of the rotor pole arc is increased by the saturation effect.



(a) Inductance profiles



(b) Torque characteristics

Fig. 9. Inductance and torque characteristics of the proposed 4/2 SRM

Fig. 10 shows the compared output torque characteristics of three types of 4/2 SRM. As shown in the figure, the proposed type has lower torque ripple compared to the ripples of other types. In the commutation region, the torque overlap region between two phases can supply a

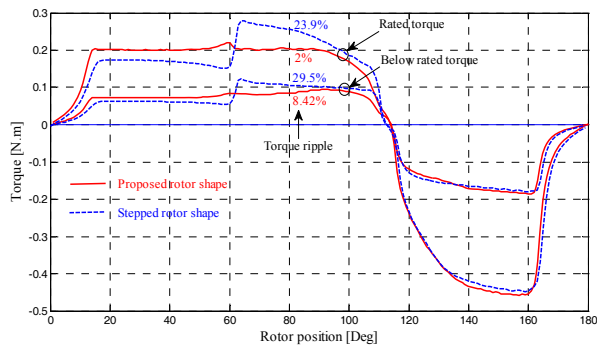


Fig. 10. Torque characteristics comparison

continuous torque without any torque dead zone. The analyzed torque ripple is under 2[%], which is the objective target value in the optimization algorithm. The torque ripple of the modified type is over 20[%] at the rated torque.

Fig. 11 shows the efficiency and loss characteristics of the designed motor by the mathematical simulation model. The efficiency does not include mechanical loss and windage loss. The maximum efficiency is about 89[%] at the rated speed.

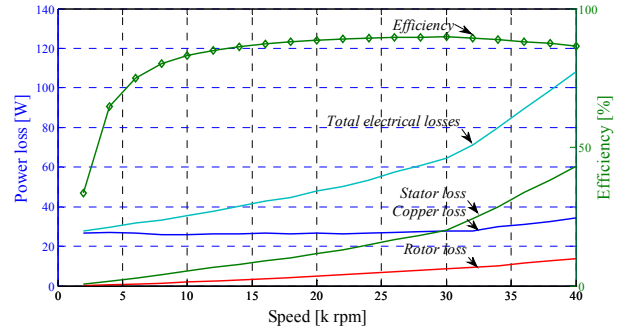


Fig. 11. Simulated efficiency and loss characteristics

4. Experimental Results

The prototype motor is manufactured to verify the proposed high-speed 4/2 SRM, The 35PN210 (POSCO) steel is used to manufacture the rotor and the stator.

Fig. 12 shows the experimental configurations. The main controller is designed by TMS320F2811-150MHz from Texas Instrument. The rotor position is detected by a non-contactable magnet sensor, which can supply 4096 pulses per revolution. The non-contactable magnet position sensor is very useful in the high-speed application due to the bearingless and nonmechanical friction. The position pulses are captured by the QEP module, which is an embedded function of the Digital Signal Processor (DSP). ACS720 chip-type current sensor for automotive and 12-bit ADC module of DSP are used to detect phase current. A simple power FET with a 600[V], 30[A] rate is used for the



Fig. 12. Experimental configurations

asymmetric converter. For the load test and power analysis, high-speed dynamometer 2WB43 with 50,000[rpm] maximum speed and power analyzer PPA2530 are used.

Fig. 13 shows the measured torque characteristics of the prototype motor. It has higher torque ripple than expected due to manufacturing error in the rotor and stator. From the practical measurement, the rotor dimensions have 1[%] diameter error in region 1 and 0.7[%] diameter error in region 3. Furthermore, the assembly of the stator and the bracket has distortion in the rotational direction. This distortion makes a concentricity error between stator and rotor assembly. As such, the measured torque has an error with the analyzed torque. However, the prototype motor has a wide torque region with phase overlap. It develops a continuous torque in the practical air blower without any torque dead zone.

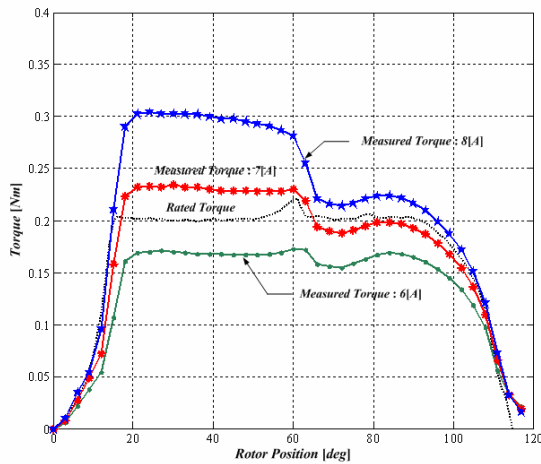


Fig. 13. Measured torque characteristics



Fig. 14. Measured torque characteristics

Fig. 14 shows the measured torque of the practical air blower with the impeller. As shown in the figure, the proposed control scheme maintains the reference speed well, reaching the target speed in 1.5[s] without any oscillation.

Fig. 15 shows the total efficiency of the motor and the drive with output power. The maximum driving efficiency

is 72.2[%]. Mechanical loss in the bearing and windage loss are not considered. In the low-speed region, the measured efficiency is similar to the expected one. However, the efficiency is lower in the high-speed region due to mechanical loss and windage loss. In comparison with a conventional universal motor applied using the same application, the efficiency of the prototype motor is 7[%] higher than that of a conventional one.

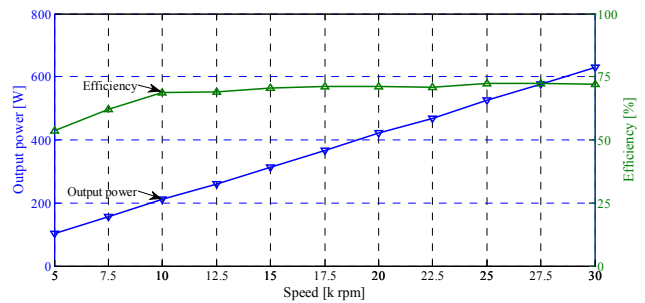


Fig. 15. Measured output power and drive efficiency

5. Conclusion

The current study presents the design and characteristics of a prototype high-speed 4/2 SRM with a comparative study of some conventional high-speed motors. The prototype motor is designed based on the continuous stepper-type rotor because of its simple structure, and the rotor shape is optimized by the reiterative FEM calculation to reduce torque ripple. The optimized rotor shape has a long uniform, a short uniform, and a non-uniform air-gap region. The torque ripple at the rated torque is satisfied. Moreover, the positive torque region is wider than a conventional 4/2 SRM without any torque dead zone.

In the experimental results, the prototype motor has 72.2[%] efficiency at 30,000[rpm], and the output power is satisfied with the desired value.

Acknowledgment

This work was supported by the Energy Resource R&D program (2009T100100654) under the Ministry of Knowledge Economy, Republic of Korea.

References

[1] J. W. Ahn, T. H. Kim, D. H. Lee, "Performances of SRM for LSEV", Journal of Power Electronics, vol.5, no.1, pp. 45–54, Jan. 2005.
 [2] D.H. Lee, Z. G. Lee, L. Jianing, J.W. Ahn, "Single-Phase SRM Drive with Torque Ripple Reduction and Power Factor Correction", IEEE Trans. on Industry Applications, Vol 43, Issue 6, pp.1578–1587, Nov.–

- Dec. 2007.
- [3] K. Ohyama, M. Naguib, F. Nashed, K. Aso, H. Fujii, H. Uehara, "Design using finite element analysis of a switched reluctance motor for electric vehicle", *Journal of Power Electronics*, vol.6, no.2, pp. 163–171, April 2006.
- [4] T. Fukao, "Principles and Output Characteristics of Super High Speed Reluctance Generator Systems", *IEEE Trans. on Industry Applications*, Vol. IA-22, No. 4, PP. 702–707, 1986.
- [5] J. Faiz, J.W. Finch, H.M.B Metwally, "A novel switched reluctance motor with multiple teeth per stator pole and comparison of such motors", *Electric Power Systems Research*, ELSEVIER, vol.34, pp. 197–203, 1995.
- [6] T. Genda, H. Dohmeki, "Characteristics of 4/2 Switched Reluctance Motor for a high speed drive by the excitation angle," *Electrical Machines and Systems*, 2009. ICEMS 2009. International Conference, pp.1–6, 15–18 Nov. 2009.
- [7] Jong-Han Lee, Eun-Woong Lee, Jun-Ho Kim, "Design of the single phase SRM for the blower considering self-starting," *Electrical Machines and Systems*, 2005. ICEMS 2005. Proceedings of the Eighth International Conference on , vol.1, pp. 667–670 Vol. 1, 27–29 Sept. 2005.
- [8] Y. Kano, T. Kosaka, N. Matsui, "Optimum Design Approach for a Two-Phase Switched Reluctance Compressor Drive," *Industry Applications*, IEEE Transactions on , vol.46, no.3, pp.955–964, May–June 2010.
- [9] Qiang Zhou, Chuang Liu, Wenyu Zeng, Diji Liu, "Maximization of starting torque of a three-phase 6/2 switched reluctance motor for super high speed drive," *Electrical Machines and Systems*, 2008. ICEMS 2008. International Conference on, pp.3385–3388, 17–20 Oct. 2008.
- [10] S.I. Nabeta, I.E. Chabu, L. Lebensztajn, J.R. Cardoso, D.A.P. Correa, W.M. da Silva, "Kriging Models and Torque Improvements of a Special Switched Reluctance Motor," *Electric Machines & Drives Conference*, 2007. IEMDC '07. IEEE International, vol.1, pp.559–563, 3–5 May 2007.
- [11] V. Prabhakar, M. Balaji, S. Ramkumar, V. Kamaraj, "Influence of stator and rotor profiles on torque ripple minimization in SRM," *Power Electronics*, 2006. IICPE 2006. India International Conference, pp.403–406, 19–21 Dec. 2006.
- [12] T. Higuchi, J. O. Fiedler, R.W De Doncker, "On the design of a single-phase switched reluctance motor," *Electric Machines and Drives Conference*, 2003. IEMDC'03. IEEE International, vol.1, pp. 561–567 vol.1, 1–4 June 2003.
- [13] Seok-Gyu Oh, R. Krishnan, "Two Phase SRM With Flux Reversal Free Stator: Concept, Analysis, Design and Experimental Verification," *Industry Applications Conference*, 2006. 41st IAS Annual Meeting. Conference Record of the 2006 IEEE, vol.3, no., pp.1155–1162, 8–12 Oct. 2006.
- [14] M. Kowol, P. Mynarek, D. Mrochen, "The electromagnetic field calculation of the switched reluctance motor," *Electrodynamics and Mechatronics*, 2009. SCE 11 '09. 2nd International Students Conference on , pp.13–14, 19–21 May 2009
- [15] H. Kuss, T. Wichert, B. Szvmanski, "Design of a high speed Switched Reluctance Motor for spindle drive," *Compatibility in Power Electronics*, 2007. CPE '07, pp.1–5, May 29 2007–June 1 2007



Jin-Woo Ahn was born in Busan, Korea, in 1958. He received his B.S., M.S., and Ph.D. degrees in Electrical Engineering from Pusan National University, Busan, Korea, in 1984, 1986, and 1992, respectively. He has been with Kyungsoo University, Busan, Korea, since 1992 as a professor in the Department of Mechatronics Engineering. He is a fellow of the Korean Institute of Electrical Engineers, a member of the Korean Institute of Power Electronics, and a senior member of the Institute of Electrical and Electronics Engineers. He is the Chairman of the Academic Committee of KIEE and the vice president of the Korea Regional Innovation System Association.



Dong-Hee Lee was born on November 11, 1970. He received his B.S., M.S., and Ph.D. degrees in Electrical Engineering from Pusan National University, Busan, Korea in 1996, 1998, and 2001, respectively. He worked as a Senior Researcher for the Servo R&D Team at OTIS-LG from 2002 to 2005. Since 2005, he has been with Kyungsoo University, Busan, Korea as an assistant professor in the Department of Electrical and Mechatronics Engineering. He has served as director of the Advance Electric Machinery and Power Electronics Center since 2009. His current research interests are servo systems and electrical motor drives with power electronics.